LANGMUIR

Article

pubs.acs.org/Langmuir

Dust Effects on Nucleation Kinetics and Nanoparticle Product Size Distributions: Illustrative Case Study of a Prototype Ir(0)$_n$ Transition-Metal Nanoparticle Formation System

Saim Özkar[†] and Richard G. Finke*[,‡]

[†]Department of Chemistry, Middle East Technical University, 06800 Ankara, Turkey

[‡]Department of Chemistry, Colorado State University, Fort Collins, Colorado 80523, United States

Supporting Information

ABSTRACT: The question is addressed if dust is kinetically important in the nucleation and growth of Ir(0)$_n$ nanoparticles formed from $[Bu_4N]_5Na_3(1,5\text{-COD})Ir^I{\cdot}P_2W_{15}Nb_3O_{62}$ (hereafter $[(COD)Ir{\cdot}POM]^{8-}$), reduced by H_2 in propylene carbonate solvent. Following a concise review of the (often-neglected) literature addressing dust in nucleation phenomena dating back to the late 1800s, the nucleation and growth kinetics of the $[(COD)Ir{\cdot}POM]^{8-}$ precatalyst system are examined for the effects of 0.2 μm microfiltration of the solvent and precatalyst solution, of rinsing the glassware with that microfiltered solvent, of silanizing the glass reaction vessel, for the addition of <0.2 μm γ-Al_2O_3 (inorganic) dust, for the addition of flame-made carbon-based (organic) dust, and as a function of the starting, microfiltered $[(COD)Ir{\cdot}POM^{8-}]$ concentration. Efforts to detect dust and its removal by dynamic light scattering and by optical microscopy are also reported. The results yield a list of eight important conclusions, the four most noteworthy of which are (i) that the nucleation apparent rate "constant" $k_{1obs(bimol)}$ is shown to be slowed by a factor of ~5 to ~7.6, depending on the precise experiment and its conditions, just by the filtration of the precatalyst solution using a 0.20 μm filter and rinsing the glassware surface with 0.20 μm filtered propylene carbonate solvent; (ii) that simply employing a 0.20 μm filtration step narrows the size distribution of the resulting Ir(0)$_n$ nanoparticles by a factor of 2.4 from ±19 to ±8%, a remarkable result; (iii) that the narrower size distribution can be accounted for by the slowed nucleation rate constant, $k_{1obs(bimol)}$, and by the unchanged autocatalytic growth rate constant, $k_{2obs(bimol)}$, that is, by the increased ratio of $k_{2obs(bimol)}/k_{1obs(bimol)}$ that further separates nucleation from growth in time for filtered vs unfiltered solutions; and (iv) that five lines of evidence indicate that the filterable component of the solution, which has nucleation rate-enhancing and size-dispersion broadening effects, is dust.

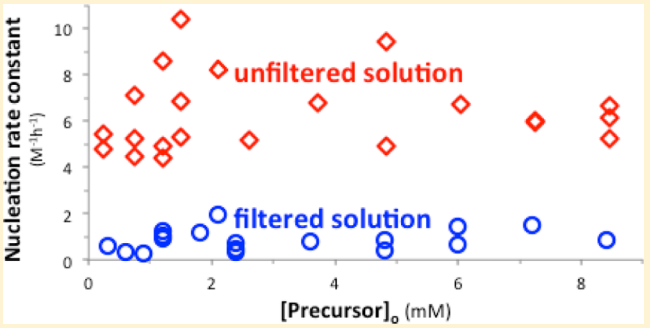

INTRODUCTION

Nucleation is a critical self-assembly, phase-change process that is omnipresent throughout nature.[1−6] Nucleation is the key initial step in the formation of natural, condensed systems as diverse as cloud, rain, and snow formation; protein aggregation in neurological diseases; liquid to solid crystallizations; pattern formation including the formation of bones, teeth, and sea shells; and nanoparticle formation in catalysis or other areas of materials chemistry, to pick from among many more known examples.[1−6]

Prototype Ir(0)$_{\sim 300}$ Nanoparticle Nucleation and Growth System. Nucleation in the present case of Ir(0)$_{\sim 300}$ transition-metal nanoparticle formation, shown in the net reaction provided in Scheme 1, involves precursor **A** = $[Bu_4N]_5Na_3(1,5\text{-COD})Ir^I{\cdot}P_2W_{15}Nb_3O_{62}$ (hereafter abbreviated as $[(COD)Ir{\cdot}POM]^{8-}$, where POM^{9-} is the nanoparticle-stabilizing[7] polyoxometalate polyanion,[8,9] $P_2W_{15}Nb_3O_{62}{}^{9-}$). The nanoparticle formation reaction in Scheme 1 involves the $\{(1,5\text{-COD})Ir^I\}^+$ organometallic component being reduced from Ir(I) to Ir(0) by 0.5 equiv of H_2. The normal result is a relatively narrow dispersion of 2.0 ± 0.3 nm diameter Ir$_{\sim 300}$ nanoparticles with surface-attached, stabilizing POM^{9-} polyanions,[7,9] with a ±15% "near monodisperse"[10] dispersion referring to the normal use heretofore of unfiltered solutions in the synthesis. No size dispersion below this ±15% value has been seen prior to the current work and despite more than 1000 kinetic experiments to date with the $[(COD)Ir{\cdot}POM]^{8-}$

Scheme 1. Stoichiometry of Formation of Ir(0)$_{\sim 300}$ Nanoparticles from $[(1,5\text{-COD})Ir{\cdot}P_2W_{15}Nb_3O_{62}]^{8-}$ under Hydrogen

$$300\ [(1,5\text{-COD})Ir{\bullet}P_2W_{15}Nb_3O_{62}]^{8-} + 750\ H_2 \longrightarrow 1\ Ir(0)_{\sim 300} + 300\ [P_2W_{15}Nb_3O_{62}]^{9-} + 300\ \bigcirc + 300\ H^+$$

Received: April 20, 2017
Revised: May 31, 2017
Published: June 22, 2017

DOI: 10.1021/acs.langmuir.7b01219
Langmuir 2017, 33, 6550−6562

system and TEM, HR-TEM, or HAADF-STEM examination of the $Ir(0)_n$ reaction products.

The minimum kinetic model able to account for the kinetic data typically observed for the reaction in Scheme 1 is the two-step, first-order nucleation and then autocatalytic growth mechanism known as the (first-order nucleation) Finke–Watzky mechanism, $\mathbf{A} \rightarrow \mathbf{B}$ (rate constant k_1) then $\mathbf{A} + \mathbf{B} \rightarrow 2\mathbf{B}$ (rate constant k_2),[11] where again **A** is the $(COD)Ir{\cdot}POM^{8-}$ precatalyst and **B** is Ir(0) in the growing nanoparticle. Significantly, in recent work[12] nucleation was shown to actually be net second order in **A**, $\mathbf{A} + \mathbf{A} \rightarrow 2\mathbf{B}$ (rate constant $k_{1obs(bimol)}$). The kinetics and mechanism for the ~300 $[(COD)Ir{\cdot}POM]^{8-}$ to 1 $Ir(0)_{\sim 300}$ nanoparticle formation system consist, then, primarily of a two-step mechanism of slow, continuous second-order nucleation[12] and then autocatalytic surface growth,[11] although a smaller nanoparticle, **B**, bimolecular agglomeration[13−21] ($\mathbf{B} + \mathbf{B} \rightarrow \mathbf{C}$) to larger nanoparticles, **C**, and autocatalytic agglomeration between smaller and larger nanoparticles ($\mathbf{B} + \mathbf{C} \rightarrow 1.5\mathbf{C}$) are also now well-established and round out the more general, overall four-step mechanism for nanoparticle formation.[13] The $[(COD)Ir{\cdot}POM]^{8-}$ nanoparticle precatalyst and formation system is as well studied[11,12,22] as any other single nucleation, growth, and agglomeration system. One of the important conclusions reached recently[12] is that classical nucleation theory and its implied reversible, thermochemically controlled, higher-molecularity nucleation process of $n\mathbf{A} \rightleftharpoons \mathbf{A}_n$ is disproven for at least the nucleation of the $Ir(0)_n$ transition-metal nanoparticles in Scheme 1. Also discussed as part of that prior work[12] is why classical nucleation theory[23−28] is likely best viewed as inapplicable to most other non-gas-phase, more strongly bonding systems in nature.

Nucleation Termolecular in Ir Hides under Second-Order Kinetics in A, Plus the Lack of Any Parallel Path Heterogeneous Nucleation. In our most recent study, nucleation was shown to actually be termolecular in Ir (i.e., Ir_3)[22] with what we define as the Kinetically Effective Nucleus (KEN)[12] determined to be of nominal composition $\{Ir_3H_{2x}POM\}^{6-}$.[22] Of direct relevance to the present work, the intercept of a k_{1obs} ($= k_{1obs(bimol)}[\mathbf{A}]$) vs [**A**] plot as part of that prior study went through the origin with a *y* intercept of zero within experimental error (*y* intercept = $(1.3 \pm 3.8) \times 10^{-3}$ h^{-1}), indicating that no parallel-path heterogeneous or other (parallel-path) nucleation is seen in the $Ir(0)_{\sim 300}$ nanoparticle formation system, the key word here being parallel path as discussed more in our prior publication.[12] However, recognized but not answered as part of that prior study is the question of whether any heterogeneous nucleation of any type is involved in the formation of the $\{Ir_3H_{2x}POM\}^{6-}$ kinetically effective nucleus.

Relevant Key Literature of Heterogeneous Nucleation. It is well established that heterogeneous nucleation, that is, nucleation involving glass or other surfaces, dust, or other dispersed but nonsoluble, "heterogeneous" phases,[29] is typically faster in most systems than arguably rare, true homogeneous nucleation.[30]

Early 1880s Reports on the Role of Airborn Particles in Water Condensation. Coulier and Aitken have reported the results of the first experiments showing the role of the airborne particles in vapor condensation processes.[31−37] Of particular interest is their experiment demonstrating that in a dust-free glass flask water vapor can condense only when either dirty, dust-containing air or carbon dust made by an acetylene flame is introduced. Also classic here are Aitken's design and the use of a simple apparatus for counting the number of dust particles in different atmospheres,[31−37] estimating at the time that the number or particles in clear outside air and air inside rooms, although quite variable, often ranges from $\sim 10^{4-5}$ to $\sim 10^{5-6}$ particles per cm^3, respectively.[35]

Turkevich et al.'s Study of Colloidal Gold. A short statement in the pioneering 1951 paper on colloidal gold formation by Turkevich et al. notes that[38] "In the absence of nuclei and in a dust-free atmosphere the growth medium undergoes no reduction of the auric ion for several hours." Hence, in this early, little-cited aspect of Turkevich et al.'s classic work, the importance of dust in the formation of colloidal gold is clearly noted, albeit nearly completely ignored since then. However, no detailed mechanistic insights were available at the time from which to understand more deeply the mechanistic step(s) affected by the presence of dust.

Matijević et al.'s Study of Sulfur Sols. A seminal 1963 paper[39] reports the results of a study on the size distribution of sulfur sols obtained following a modified LaMer[40] procedure whereby careful attention to the purity of the starting reagents, the water solvent, efficient mixing, temperature control, and the removal of dust by the use of a 0.22 μm microfilter was reported by Matijević and co-workers as necessary to achieve a reproducible synthesis of S_n sols. Significantly, that careful experimental work narrowed the final size distribution 2-fold for 95% of the observed particles to 0.48 ± 0.04 μm (i.e., ± 8%)[39] from that seen of 0.51 ± 0.08 μm (i.e., ±16%) in an earlier,[41] ostensibly closely analogous synthesis.[39] However, it was unrecognized—and in fairness to the authors of that classic 1963 study, unrecognizable at the time—that the elimination of dust was probably a major factor in the observed 2-fold narrowing of the particle size distribution, an interpretation suggested on the basis of the results obtain herein, vide infra.

State-of-the-Art Crystallization Kinetics Study by Kulkarni and Coworkers. A recent state-of-the-art crystallization kinetics nucleation study of an organic compound is shown in Scheme 2, from a paper once again quite relevant to the present study.[42]

Scheme 2. Heating and Cooling Cycle for the Crystallization of Isonicotinamide (INA) from Supersaturated Solution

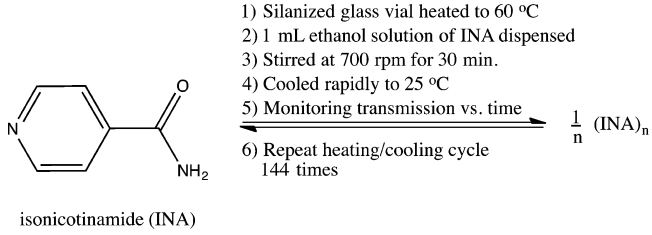

As Scheme 2 shows, isonicotinamide at supersaturating concentrations was heated and then cooled, whereas a loss from 100% transmissivity of the initially clear-when-hot solution was monitored as crystallization ensued (with an implied ±3% error in the transmissivity from examining Figure 1 in that work[42]). The heating–cooling cycle was repeated 144 times for each solution, yielding as much and as precise crystallization kinetic data as one will find in the literature. The data were analyzed by assuming that nucleation is stochastic (i.e., probabilistic) and then analyzing the data with a nonmechanistic, empirical nucleation rate, *J*, model, $J(S) = A{\cdot}S\exp(-B/\ln^2 S)$, where *S* is the supersaturation and *A* and *B*

DOI: 10.1021/acs.langmuir.7b01219
Langmuir 2017, 33, 6550−6562

are kinetic and nucleation rate parameters.[42] The authors find what they call the nucleus size to be n^* 11−50, that is, $(\text{isonicotinamide})_{11-50}$, although the authors are really measuring what we have recently termed the first observable cluster (FOC),[12] not the fundamentally more interesting kinetically effective nucleus (that should be ≪11−50).[42] The assumption of stochastic nucleation and the empirical (rather than the desired mechanistic) model of nucleation limit the mechanistic value, but not the fundamental importance, of the state-of-the-art work by Kulkarni and co-workers.

The Kulkarni et al. paper also reports the important finding that the empirical nucleation rate, J (really the rate of formation of the FOC monitored by a decrease in the intensity of transmitted light), for a supersaturation of S = 1.44 in a silanized glass reactor is 631 ± 9 m^{-3} s^{-1} (i.e., ± 1.4%) for unfiltered solutions. That rate, J, drops 2.7-fold to 233 ± 12 m^{-3} s^{-1} (i.e., ± 5.1%) for solutions simply filtered through a 0.45 μm membrane filter. The difference is attributed to room dust by the authors, although direct evidence for dust, including the size or type of the dust (i.e., inorganic and/or organic) and hence compelling evidence for its removal by the filtration step, is lacking. Nevertheless, Kulkarni et al.'s study is currently state-of-the-art and provides further literature precedent at least consistent with heterogeneous nucleation due to room dust in at least what we call weakly associating systems[12] (i.e., systems with intrinsically weaker intermolecular interactions than, for example, the much stronger, ca. ≥26 kcal/mol Ir(0)−Ir(0) bonds formed in $Ir(0)_n$ nanoparticles).[12] Another intriguing insight from the study of Kulkarni and coworkers is that the error bars in the rate of loss of transmitted light are 5.1%/1.4% = 3.6 fold smaller (i.e., a smaller relative error) in the unfiltered solutions. That is, the unfiltered solution provides more precise kinetic data, at least in this particular organic crystal system, a result that we will find is also seen for the nucleation rate constants obtained herein for our $Ir(0)_n$ nanoparticle formation system.

Mineral (Inorganic) Dust in Atmospheric Nucleation Processes. Dust-mediated nucleation is perhaps best studied via atmospheric chemistry where mineral dust is implicated in contributing to ice nucleation within clouds, for example,[43] and dates back to the classic late 1800 studies of Coulier and Aitken.[31−36] Atmospheric dust contains minerals such as quartz or calcite or minerals that are basically aluminosilicates such as illite, kaolinite, montmorillonite, or silicates (Table 1).[43] Mixtures of minerals such as Arizona test dust (ATD) are also well known and have been studied in atmospheric nucleation.[43] The most relevant part to the present work is that even a bit of reading in the area of dust-mediated nucleation in atmospheric chemistry gives one an appreciation for the complexity and heterogeneity involved in the term dust, not to mention its relatively little studied effect(s) on nucleation.

Table 1. Chemical Components of Atmospheric Inorganic Dust According to XRD Analysis[43]

mineral	chemical formula
quartz	SiO_2
calcite	$Ca(CO_3)$
albite	$Na(Si_3Al)O_8$
orthoclase	$KAlSi_3O_8$
illite1	$KAl_2(Si_3Al)O_{10}(OH)_2$
illite2	$(K,H_{30})Al_2(Si_3Al)O_{10}(OH)_2{\cdot}xH_2O$
montmorillonite	$(Ca,Na)_{0.3}Al_2(Si,Al)_4O_{10}(OH)_2{\cdot}xH_2O$
anorthite	$(Ca,Na)(Al,Si)_2Si_2O_8$

Interestingly, our literature search found little on organically or biologically based dust in nucleation processes[44,45] since the time of Couiler and Aitken's classic studies, which cited the effects of acetylene flame soot on water-vapor condensation.[31−36] However, a recent *C&EN News* article[46] focused on an ever-growing list of organic contaminants in (organic) dust and on the research efforts to understand what these compounds and such nontraditional, organic dusts mean for human health or, for example, the nucleation and growth of particles throughout nature.

Focal Points of the Present Study. *Possibility of Heterogeneous Nucleation in $Ir(0)_n$ Nanoparticle Formation.* The key set of questions asked, and hence the focal points of the present contribution, are the following: (i) Does 0.20 μm Nalgene membrane microfiltration have an effect on the nucleation and/or growth kinetics of the $Ir(0)_{\sim 300}$ nanoparticle formation system described in Scheme 1, where its nucleation has recently been found[22] to be termolecular in Ir and involves the hydrogen reductant in an implied kinetically effective nucleus (KEN) of $\{Ir_3H_{2x}POM\}^{6-}$? (ii) Are the size and size distribution of the resultant $Ir(0)_n$ nanoparticles influenced by such filtration? (iii) If filtration effects are seen on either the kinetics or size/size distribution, what alternative explanations including possible artifacts are conceivable, and can they be disproved? For example, could the membrane filter just be removing some $[(COD)Ir{\cdot}POM]^{8-}$ components, thereby causing any change in rate that might be seen postmicrofiltration? Could some soluble component of the Nalgene membrane conceivably be serving as a rate-changing poison or accelerant, depending on what is observed post microfiltration? (iv) Do complementary light scattering or optical microscopy studies support or refute the involvement of room dust in the unfiltered vs filtered solutions? (v) Is dust or other heterogeneous nucleation the reason behind the ±50−200% error in individual nucleation, k_{1obs}, rate constants in even our best data,[12] data where we worked hard[12] to bring down the error to that level from a prior maximum of $\sim 10^{\pm 1.2}$ (i.e., 1585%!) interinvestigator error[47] to a relatively small 50−200%[12] single-investigator error for the system in Scheme 1? It is noteworthy here that precise, homogeneous nucleation rate constants are notoriously hard to measure, in part because heterogeneous nucleation is typically more facile[30] and arguably (vide infra) omnipresent. Additionally, (vi) what are the effects if any of deliberately added inorganic or organic dust? Finally, (vii) if evidence for the kinetic effects of dust is observed, is then $\{(Ir_3H_{2x}POM^{6-}){\cdot}\text{dust}\}$ the implied, true minimal KEN of ostensibly homogeneous nucleation and growth systems such as the prototypical well-studied $Ir(0)_n$ formation system in Scheme 1? Hence, by implication and in light of the extant literature,[31−36,38,39,42] is dust likely involved in many if not most other nucleation systems throughout nature? Are the classic 1880s studies of Coulier and Aitken,[31−36] the 2013 studies of Kulkarni and co-workers,[42] and now the present study of a prototypical $Ir(0)_n$ nanoparticle formation system examples of the role of dust that a wide range of scientists studying nucleation, growth, and agglomeration phenomena across nature must take into account in the future?

DOI: 10.1021/acs.langmuir.7b01219
Langmuir 2017, 33, 6550−6562

RESULTS AND DISCUSSION

Initial Studies of Microfiltration Effects on the Nucleation and Growth Kinetics of the $[Bu_4N]_5Na_3(1,5\text{-COD})Ir\cdot P_2W_{15}Nb_3O_{62}$ to $Ir(0)_n$ Nanoparticle Formation System. A typical nucleation and growth kinetics curve,[8,11−13,22] when beginning with 1.2 mM **A** = $[Bu_4N]_5Na_3(1,5\text{-COD})Ir\cdot P_2W_{15}Nb_3O_{62}$ in propylene carbonate under an initial 40 psig H_2 and at 22.0 ± 0.1 °C, is shown in Figure 1 (blue squares, □). The reaction is monitored by our well-precedented cyclohexene hydrogenation catalytic reporter-reaction method[8,11,12,22] shown in Scheme 3. Note that because nucleation for this $Ir(0)_n$ nanoparticle formation system has been shown to be second order in [**A**],[12] we use the second-order FW two-step mechanism of **A** + **A** → **B** (rate constant $k_{1obsd(bimol)}$) and **A** + **B** → 2**B** (rate constant $k_{2obsd(bimol)}$) to fit the kinetics data, which in turn yields $k_{1obs(bimol)}$ for the nucleation step.[48] Fitting the sigmoidal curve to the integrated rate equation[12] corresponding to the second-order nucleation FW two-step mechanism was accomplished using nonlinear least-squares,[12] and the result is shown in Figure 1 (blue curve and squares, □).

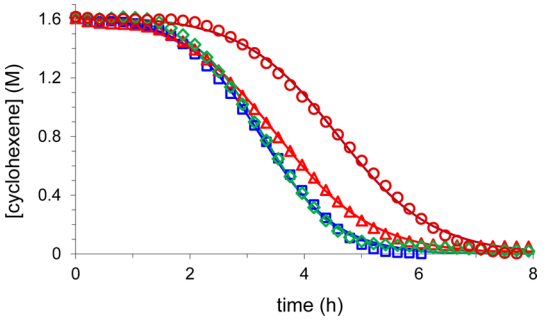

Figure 1. Nucleation and growth kinetic data obtained by the catalytic reporter reaction method shown in Scheme 3 (i) when beginning with 1.2 mM $[Bu_4N]_5Na_3(1,5\text{-COD})Ir\cdot P_2W_{15}Nb_3O_{62}$ in propylene carbonate under an initial 40 psig H_2 and at 22.0 ± 0.1 °C (blue squares, □); (ii) under the same conditions but now with the solution filtered through a 0.20 μm Nalgene syringe filter and the reaction vessel rinsed with the filtered propylene carbonate (dark-red circles, ○); (iii) under the same conditions but now with just the solution filtered through a 0.20 μm Nalgene syringe filter without rinsing the glassware with the filtered propylene carbonate solvent (green diamonds, ◊); and (iv) under the same conditions but now with just the reaction tube rinsed with the filtered propylene carbonate solvent while using the unfiltered reaction solution (red triangles, Δ). The nonlinear least-squares curve fitting of the data employs the integrated rate equation[12] corresponding to the two-step, second-order nucleation and then autocatalytic growth mechanism **A** + **A** → 2**B** (rate constant $k_{1obs(bimol)}$), **A** + **B** → 2**B** (rate constant $k_{2obs(bimol)}$).[11,12] Note that only one of every five data points collected is shown for clarity.

When the nanoparticle formation reaction is performed under the same conditions but now starting with the precatalyst solution filtered through a 0.20 μm Nalgene syringe filter directly into the reaction vessel (which was prerinsed with the filtered propylene carbonate solvent to remove as much dust as possible), one obtains a similar but significantly slower nanoparticle formation kinetic curve (Figure 1, dark-red circles, ○). Those kinetic data are also well fit by the second-order nucleation FW two-step mechanism, yielding the rate constants $k_{1obs(bimol)}$ for the nucleation (**A** + **A** → 2**B**) and $k_{2obs(bimol)}$ for the autocatalytic growth (**A** + **B** → 2**B**) (Table 2).[12] Hence,

Scheme 3. Second-Order Nucleation FW Two-Step Mechanism and How It Is Conveniently Monitored by Coupling It to the Well-Established,[8,11−13,22] Fast Cyclohexene Hydrogenation Reporter Reaction[a]

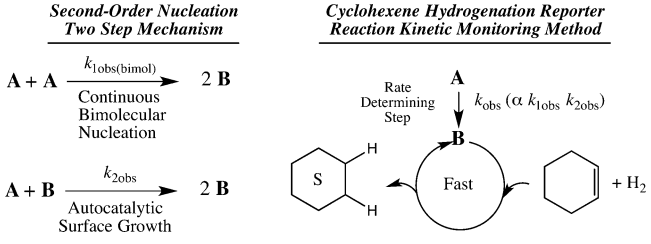

[a]**A** is $[(Bu_4N)_5Na_3(1,5\text{-COD})Ir\cdot P_2W_{15}Nb_3O_{62}]$, and **B** is the growing, averaged $Ir(0)_n$ nanoparticle.

Table 2. Nucleation and Growth Kinetics Data, as a Function of the Initial Concentration of $[A]_o = [(COD)Ir(POM)]_o = [(1,5\text{-COD})Ir\cdot P_2W_{15}Nb_3O_{62}^{8-}]_o$, Beginning with Filtered or Unfiltered Precatalyst Solution Plus 0.5 mL of Cyclohexene in Propylene Carbonate under an Initial 40 psig H_2 and at 22.0 ± 0.1 °C

	$k_{1obs(bimol)}$ (h^{-1} M^{-1})		$k_{2obs(bimol)}$ (h^{-1} M^{-1})	
$[A]_o$ (mM)	unfiltered solution	filtered solution	unfiltered solution	filtered solution
0.25	4.8		1540	
	5.4		2030	
0.30		0.63		930
0.60		0.32		1300
0.75	7.1		1300	
	5.2		1800	
	4.5		1470	
0.90		0.26		2400
1.2	4.9	1.1	1300	2200
	8.6	1.3	1200	1330
	4.4	0.92	2060	2200
1.5	10.4		880	
	5.3		1840	
	6.9		870	
1.8		1.2		1740
2.4		0.75		690
		0.31		750
		0.46		1440
2.61	5.2		760	
3.6		0.78		550
3.73	6.8		690	
4.8		0.88		480
		0.43		990
4.84	9.4		510	
	4.9		550	
6.0		0.64		470
		1.4		660
6.04	6.7		280	
7.2		1.5		300
7.25	6.0		300	
	5.9		210	
8.4		0.88		550
8.45	6.1		210	
	5.3		160	
	6.7		220	

DOI: 10.1021/acs.langmuir.7b01219
Langmuir 2017, 33, 6550−6562

upon filtration nucleation rate constant $k_{1obs(bimol)}$ is reduced from 4.9 to 1.1 M^{-1} h^{-1}, implying that removal of the filterable component present in the system slows the nucleation by nearly 5-fold. To obtain the observed rate decrease, both the filtration of the precatalyst solution through a 0.20 μm Nalgene syringe filter *and* rinsing the reaction glass with the filtered solvent are required. Neither of the filtration of the precatalyst solution nor the rinsing the reaction vessel with the filtered propylene carbonate solvent alone yields any significant change in the nucleation kinetics, as Figure 1 demonstrates.

Control of Employing Silanized but Unrinsed Glass Reaction Vessels with Filtered Solutions. Silanized glass reaction vessels have been used to prevent glass surface heterogeneous nucleation in the study on crystal nucleation kinetics of isonicotinamide from ethanol in glass vials.[42] Hence, we prepared and employed a silanized glass reactor as a control designed to test for glass-surface heterogeneous nucleation in the formation of $Ir(0)_n$ nanoparticles starting with filtered and unfiltered precatalyst solutions.

What we observed is that using a silanized glass reactor has no detectable effect on the $Ir(0)_n$ nanoparticle formation kinetics in comparison to using the normal, unsilanized glass vessel (Figure S1 in the SI). This observation indicates that the heterogeneous nucleation we are observing is not due to the glass surface. This is fully consistent with the control we did back in 1997 of showing that a 2.5-fold excess of glass surface area, added to the reaction vessel in the form of glass beads, had no detectable effect on the reaction or its kinetics. (See footnote 43(a) in ref 11.)

To summarize, then, the filtration studies in Figure 1 and the other evidence to this point support the presence of a filterable component that is present in solution and on glassware surfaces. Both must be removed to see the full, nearly 5-fold slowing effect (Table 2) that filtration through a 0.20 μm Nalgene syringe filter has on the nucleation rate constant for the $Ir(0)_n$ nanoparticle formation system.

Studies of the Effects of Microfiltration on Kinetics as a Function of the Starting $[Bu_4N]_5Na_3(1,5\text{-COD})Ir\cdot P_2W_{15}Nb_3O_{62}$ Precursor Concentration. To test more rigorously and to provide a more precise value of the nucleation-slowing effect of filtering the solutions, studies of the effects of 0.2 μm microfiltration were performed as a function of the starting precatalyst concentration. The same microfiltration protocol of the precatalyst solution, with rinsing the glass of the reactor with the filtered solvent, was performed prior to the nanoparticle formation reaction and cyclohexene hydrogenation reporter reaction method, but now all while employing the $[Bu_4N]_5Na_3(1,5\text{-COD})Ir\cdot P_2W_{15}Nb_3O_{62}$ precursor at different initial concentrations.

The kinetics data collected from these experiments are listed in Table 2 along with the values of the nucleation and growth rate constants obtained previously for the unfiltered solutions.[22] The nucleation rate constant $k_{1obs(bimol)}$ obtained using the filtered and unfiltered solutions was then plotted versus the initial concentration of the $[A]_o = [(1,5\text{-COD})Ir\cdot P_2W_{15}Nb_3O_{62}^{8-}]_o = [(COD)Ir(POM)]_o$ precursor complex (Figure 2).

The data, while scattered as expected (because measuring precise nucleation rate constants is always challenging[12,49]), show a clear difference between using the unfiltered vs the filtered solutions. The average values of $k_{1obs(bimol)}$ are 6.2 ± 1.7 and 0.81 ± 0.38 M^{-1} h^{-1} for the unfiltered and the filtered solutions, respectively, a ~7.6-fold rate-lowering effect of

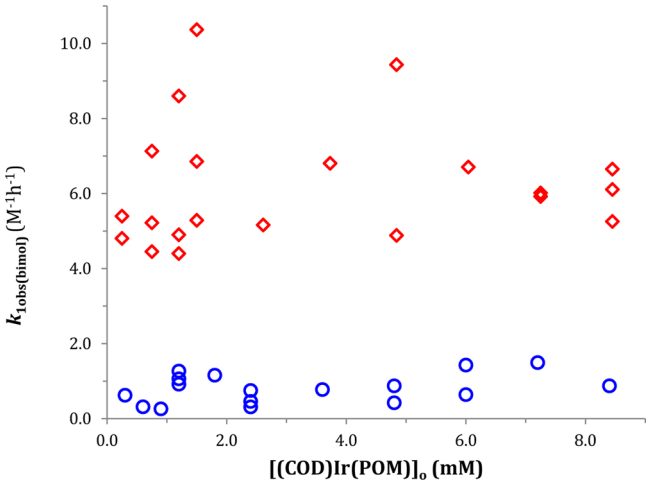

Figure 2. Plots of the nucleation rate constant $k_{1obs(bimol)}$ when beginning with filtered (blue circles, ○) or unfiltered (red diamonds, ◊) precatalyst solution of precursor $[Bu_4N]_5Na_3(1,5\text{-COD})Ir\cdot P_2W_{15}Nb_3O_{62}$ plus 0.5 mL of cyclohexene in propylene carbonate under an initial 40 psig H_2 and at 22.0 ± 0.1 °C. The $k_{1obs(bimol)}$ was obtained by nonlinear least-squares curve fitting of the data to the second-order nucleation FW 2-step mechanism,[12] corrected versus the initial concentration of precursor $[A]_o = [(COD)Ir(POM)]_o = [(1,5\text{-COD})Ir\cdot P_2W_{15}Nb_3O_{62}^{8-}]_o$ as the mathematics of the reporter reaction method requires.[11,22] The average values of $k_{1obs(bimol)}$ for the unfiltered and filtered solutions are 6.2(±1.7) and 0.81(±0.38) M^{-1} h^{-1}, respectively.

filtration on slowing the nucleation rate constant, $k_{1obs(bimol)}$. Of further interest is that the faster nucleation in the unfiltered solutions has a nearly 4.5-fold (=1.7/0.38) larger absolute error in $k_{1obs(bimol)}$ compared to that of the filtered solutions, although a 1.7-fold smaller, ±27% relative error in $k_{1obs(bimol)}$ without filtration vs the ±47% relative error in $k_{1obs(bimol)}$ with filtration (i.e., ±47%/1.7 = ±27%). One sees this latter, ostensibly the same and hence possibly more general, result in the isonicotinamide crystallization study cited in the Introduction: there the authors report 3.6-fold smaller (apparently record minimum), ±1.4% error bars for the faster nucleation rates for dye agglomeration in unfiltered solution (i.e., in comparison to the 3.6-fold larger, ±5% error bars in the nucleation rates for the filtered solutions).[42]

To summarize the studies and data to this point, we have compelling evidence that filtration affects the kinetics of nucleation of the prototype ~300 $[(COD)Ir(POM)]^{8-}$ plus 750 H_2 to 1 $Ir(0)_{\sim 300}$ nanoparticle formation system (Scheme 1, vide supra). The effect is not trivial but rather is a factor of ~7.6-fold (~760%) under the stated conditions of the reaction. The nucleation-enhancing component is filterable, and one also knows that the rate-enhancing component exists not only in solution, but also on the walls of the glass reactor because rinsing the glass surfaces with filtered solvent is required to remove the rate-enhancing component. Dust is certainly the leading candidate if not the only reasonable candidate for that filterable component, in part because people who have ever dusted any room in their house or laboratory to remove dust know that dust is omnipresent (i.e., outside of a ISO classification Clean Room[50]). However, the task remains of trying to provide more direct evidence for dust, to study the effects of deliberately added dust of some type, and to rule out any alternative hypotheses for the effects of filtration (i.e., other than the removal of dust) that could at least in principle

DOI: 10.1021/acs.langmuir.7b01219
Langmuir 2017, 33, 6550−6562

account for the observed effects of microfiltration. The needed, rare studies of attempting to directly detect dust are reported next.

Efforts at Obtaining Direct Evidence for the Presence of Adventitious Dust Plus Studies of Deliberately Added Dust. *Detection of Adventitious Dust by Light Scattering.* As noted in the Introduction, even in the best literature we have been able to locate on the effects of microfiltration and the implied dust on nucleation phenomena, direct evidence for the presence of dust (and its precise size, composition, and so on) and then for the removal of dust by microfiltration is lacking.[42] We thought that we should have at least a shot at this challenging problem, and we chose dynamic light scattering (DLS) to start because light scattering has been employed in detecting particles in plasma[51,52] or gases.[53,54] We did so with some trepidation given the expected issues of deconvoluting total light scattering by a wide range of sizes and probably shapes of low levels of broadly heterogeneous dust as well as the omnipresence of dust (e.g., on DLS instrument optics and background air) in any experiments done outside of, ideally, Class 9 Clean Room, experimental conditions.[50] Those concerns so noted, one would like to design and employ dust detection and removal experiments that others could apply in their own laboratories, ideally without the need for Clean Room conditions[50] that are presumably not readily available to most researchers and do not reflect the normal (non-Clean Room) conditions that most nanoparticle syntheses utilize.

Hence, to begin with and without employing any Clean Room or other specialized conditions, DLS was obtained on unfiltered and then microfiltered precatalyst solutions of 1.2 mM $[Bu_4N]_5Na_3(1,5\text{-COD})Ir{\cdot}P_2W_{15}Nb_3O_{62}$ plus 0.5 mL of cyclohexene in propylene carbonate (i.e., deliberately without the addition of H_2 reductant because that would have made nanoparticles, thereby making it nearly impossible to distinguish the resultant nanoparticles from dust). The 10 DLS experiments summarized in Section S1 and Figures S4 and S5 in the SI teach the following points: (i) the deconvolution of the observed total light scattering, at least with our DLS instrument, its software, and in our hands, is (not unexpectedly) not anything close to what one could call convincingly reproducible, and (ii) one needs some idea of the absolute intensities of the observed light scattering peaks seen in separate experiments (as opposed to just number (relative) % intensities) to begin to have any confidence in the interpretation of the results pre- vs postmicrofiltration. However, (iii) from the 10 total experiments, one does see evidence consistent with the removal of particles by the 0.2 μm (200 nm) microfilter although, again, the result are quite variable, even in repeat DLS scans on the identical solution. The variability seen is perhaps not unexpected given the omnipresence of dust, its heterogeneous size- and probably shape-dispersion nature, its contamination of the DLS optics and background air, and the known difficulties of deconvoluting total light scattering (i.e., deconvoluting a single autocorrelation function into its component multiple exponential decays) especially from a very broad, very heterogeneous size and shape as well as low and variable levels of adventitious (dust) particles.[55,56]

Detection of Adventitious Dust by Optical Microscopy. Because we do know that rinsing our Fischer–Porter glass bottle pressure reactor with filtered solvent is needed to remove the nucleation-enhancing filterable agent and if one postulates that dust is that main agent, then it follows that the visualization of a glass surface before and after rinsing should, at least in principle, and with the right handling methods to minimize dust recontamination, be able to visualize a reduced amount of dust on the rinsed-glass surface. For this experiment, we used 22 mm × 50 mm thin glass coverslips made for microscopy (Aldrich) stored in our drybox for 2 days (as we typically store the Fisher-Porter bottles in which the $Ir(0)_n$ nanoparticle syntheses are carried out; see the Experimental section). Three rinsed coverslips were made by rinsing with filtered solvent (and then drying and storing those glass coverslips in capped glass vials that had also been rinsed with filtered solvent to help minimize dust recontamination before the coverslips could be examined by optical microscopy). The results of optical microscopy given in Figure S6 of the SI provide evidence consistent with the removal of otherwise detectable dust particles by microfiltration of the solution and rinsing the glass with filtered solvent.

Effects of Adding Authentic Dust to a Filtered Solution. A key type of experiment when any insidious impurity is believed to be present and causes some observed effect (in this case, insidious dust[31−36,42]) is to change the amount of the hypothesized impurity to confirm or refute its anticipated effect. However, and surprisingly, experiments using any type of added authentic dust seem to be largely absent in the nucleation and growth literature, at least that outside of atmospheric chemistry, where nucleation on atmospheric dust particles has been a dominant theme since the late 1800s.[31−36,43]

Because acidic γ-Al_2O_3 has been used as a support in converting $Ir(1,5\text{-COD})Cl/\gamma\text{-}Al_2O_3$ to $Ir(0)_n/\gamma\text{-}Al_2O_3$ for a long time in our drybox (in which all samples of air-sensitive $[(COD)Ir{\cdot}POM]^{8-}$ used in these and our prior studies were prepared[57]), and because common dusts are often aluminosilicates (Table 1), we reasoned that γ-Al_2O_3 could rationally be employed as an at least initial model dust in our system. Moreover, an advantage of this model dust is that its size is known (<0.20 μm).

Hence, acidic, <0.20 μm γ-Al_2O_3 dust was added to the precatalyst solution of $[Bu_4N]_5Na_3(1,5\text{-COD})Ir{\cdot}P_2W_{15}Nb_3O_{62}$ plus cyclohexene in propylene carbonate as part of a series of control experiments. First, 8 mg of <0.20 μm γ-Al_2O_3 were placed into 3 mL total of propylene carbonate plus cyclohexene solution and briefly stirred. After letting any alumina particles settle that would over 30 min, the propylene carbonate liquid phase was transferred carefully into a glass vial and used for the preparation of the $[(COD)Ir{\cdot}POM]^{8-}$ precatalyst solution. The Experimental section can be consulted as needed for the additional details of these added <0.20 μm γ-Al_2O_3 dust experiments.

Figure 3 shows the $Ir(0)_n$ nanoparticle formation kinetics obtained with the added γ-Al_2O_3 dust in propylene carbonate under otherwise standard conditions (i.e., by 22.0 ± 0.1 °C and an initial H_2 pressure of 40 ± 1 psig) by the reporter reaction monitoring method.

Table 3 lists the values for rate constants $k_{1obs(bimol)}$ and $k_{2obs(bimol)}$. Once again, one observes that the microfiltration causes a decrease in the nucleation rate constant $k_{1obs(bimol)}$ from 4.4 to 1.1 h^{-1} M^{-1} (and therefore by a factor of ∼4 in this particular experiment), whereas no significant change is observed in growth rate constant $k_{2obs(bimol)}$ (2060 to 2140 h^{-1} M^{-1}), the unchanged $k_{2obs(bimol)}$ value serving as a kind of internal standard in the experiment and one arguing for the validity of the change observed in (just) $k_{1obs(bimol)}$. The

DOI: 10.1021/acs.langmuir.7b01219
Langmuir 2017, 33, 6550−6562

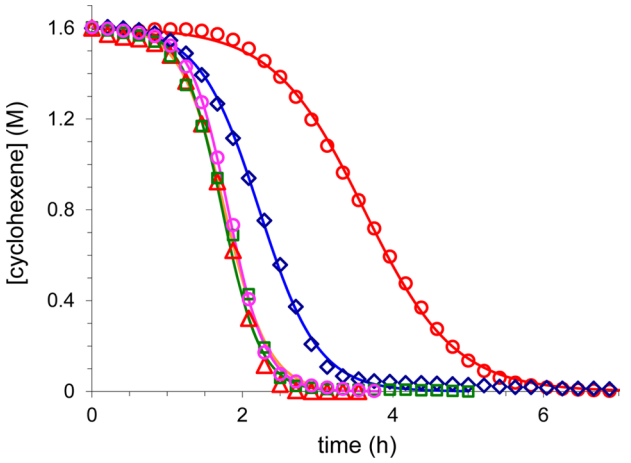

Figure 3. Nucleation and growth kinetics data when beginning with (i) unfiltered precatalyst solution of 1.2 mM $[Bu_4N]_5Na_3$(1,5-COD)Ir·$P_2W_{15}Nb_3O_{62}$ plus 0.5 mL of cyclohexene and without added γ-Al_2O_3 in propylene carbonate under an initial 40 psig H_2 and at 22.0 ± 0.1 °C (blue diamonds, ◊); (ii) under the same conditions, except now with the solution filtered through a 0.20 μm Nalgene syringe filter and the reaction vessel rinsed with the filtered propylene carbonate (red circles, ○); (iii) under the same conditions, but now with alumina (<0.20 μm in size) added to the filtered solution (red triangles, Δ); (iv) under the same conditions but now with alumina (<0.20 μm in size) added to the unfiltered solution (green squares, □); (v) under the same conditions, but now with the solution with the added alumina filtered through a 0.20 μm Nalgene syringe filter and the reaction vessel rinsed with the filtered propylene carbonate (pink circles, ○). The data are fit by nonlinear least-squares curve fitting using the integrated rate equation[12] corresponding to the two-step, second-order nucleation and then the autocatalytic growth mechanism, **A** + **A** → 2**B** (rate constant $k_{1obs(bimol)}$), **A** + **B** → 2**B** (rate constant $k_{2obs(bimol)}$).[11,12] Note that only one of every five data points collected is shown for clarity.

addition of γ-Al_2O_3 (<0.20 μm in size) dust to the unfiltered solution leads to no measurable change in the nucleation rate constant within experimental error, 4.4 vs 4.9 h^{-1} M^{-1}. However, the addition of γ-Al_2O_3 (<0.20 μm in size) dust to a filtered solution leads to an increase in the nucleation rate constant from 1.1 to 3.3 h^{-1} M^{-1} by a factor of ∼3 in that particular experiment, a nucleation rate constant nearly as large as that with natural dust, 4.9 h^{-1} M^{-1} (and likely within experimental error if one assumes a ≥±50% experimental error in $k_{1obs(bimol)}$ or if one considers that different amounts and surface areas of the (different) dusts are almost surely present). Note, unexpectedly, that a control of attempting to filter out the <0.20 μm γ-Al_2O_3 dust using a 0.2 μm filter does not remove the effect of dust on the nucleation kinetics (Figure 3 and Table 3), a control that by itself argues against any role by the Nalgene syringe microfilter and its nylon and other polymer components in causing the observed effects of using the microfiltering syringe. Additional and as mentioned in an earlier section, a second control of examining a solution to which the γ-Al_2O_3 dust had been added by DLS could not detect that added dust, the again expected result given the stated detection limit for our DLS system (60 mg/mL for particles smaller than 100 nm; we added 8 mg <0.20 μm γ-Al_2O_3 to 3 mL of solution).

However, and overall, the data are definitive in demonstrating that the addition of <0.20 μm γ-Al_2O_3 dust to a filtered precatalyst solution increases the nucleation rate in the $Ir(0)_n$ nanoparticle formation reaction to nearly that seen for the unfiltered solution, if not the same within experimental error. In short, added model dust is able to restore if not enhance the effect of removing the filterable agent. The simplest explanation of the data is that the filterable reagent is dust.

Testing if Organic Carbon-Based Dust Added to a Filtered Solution Has Any Measurable Effect. In the 1880s, Couiler and Aitken showed that water vapor rapidly condenses on carbon dust particles, which had been introduced into the system from an acetylene flame.[31−36] Hence, we added carbon dust to our filtered reaction solution by flame treatment of the reaction glass tube to determine if doing so had any measurable influence on the kinetics of Ir(0) nanoparticle formation. The experiments involved rinsing the glass tubes with the filtered propylene carbonate in a drybox and then drying them there in vacuum for 2 h before removing the glass reaction tubes from the drybox and subjecting them to a (natural-gas) Bunsen burner flame that left visible soot deposits. Optical microscopy images do show the presence of the carbon dust particles on a glass coverslip flamed the same way (Figure S7 in the SI).

However, the results in Figure S8 of the SI show that the $Ir(0)_n$ nanoparticle formation nucleation kinetics do not differ detectably when comparing a filtered solution subsequently exposed to a carbon soot vs what is seen in a control experiment using the unfiltered precatalyst solution in an unrinsed culture tube that, as a necessary step of the experiment, has been brought out of and then back into the drybox (i.e., an extra step compared to the other $Ir(0)_n$ nanoparticle catalyst formation experiments described so far). The main conclusion here seems to be that our attempts to demonstrate the effects of just organic dust on the nucleation kinetics failed, very likely because of unavoidable contamination of the glass tubes with other naturally occurring dust in the drybox, the drybox vacuum antechamber, and/or the PET

Table 3. Nucleation and Growth Kinetic Data Obtained for a Filtered or Unfiltered Precatalyst Solution of $[(COD)Ir(POM)]_o$ = $[(1,5\text{-COD})Ir{\cdot}P_2W_{15}Nb_3O_{62}^{8-}]_o$ (1.2 mM) Plus 0.5 mL of Cyclohexene and with or without Added γ-Alumina in Propylene Carbonate under an initial 40 psig H_2 and at 22.0 ± 0.1 °C[a,b,c,d]

entry	treatment of precatalyst solution $[(COD)Ir(POM)]_o$	$k_{1obs(bimol)}$ in h^{-1} M^{-1}	$k_{2obs(bimol)}$ in h^{-1} M^{-1}
1	unfiltered	3.9[b]−4.4[c]	2100[c]−2200[b]
2	filtered	0.9[b]−1.3[c]	1400[c]−2140[b]
3	γ-Al_2O_3 added to the unfiltered solution	3.4[b]−4.9[c]	2700[c]−3000[b]
4	γ-Al_2O_3 added to the filtered solution	2.0[b]−3.3[c]	3000[c]−3300[b]
5	solution filtered after the addition of γ-Al_2O_3	1.5[b]−2.1[c]	3200[c]−3500[b]

[a]The ranges given for the rate constants are based on fitting different percentages of the data so as to maximize the fit in the initial, nucleation portion. [b]From fitting 100% of the kinetic data. [c]From fitting the first 50% of the kinetic data. [d]A search for a well-defined correlation between the $k_{1obs(bimol)}$ and the $k_{2obs(bimol)}$ rate constant parameters is presented in Figure S3 of the SI, but none was found.

DOI: 10.1021/acs.langmuir.7b01219
Langmuir 2017, 33, 6550−6562

bottle used for the transportation of the tubes out of the drybox but, then, the necessary extra step of being placed back into the drybox. In short, at best these particular experiments would appear to demonstrate the difficulties in avoiding the omnipresence of dust.

Additional Support for Dust as the Filterable, Active Agent via the Disproof of the Additional Conceivable Alternative Hypotheses for the Effects of Filtering on the Nucleation Kinetics. In the end, the strongest case for dust as the active agent also requires ruling out all other conceivable, reasonably alternative hypotheses[58,59] for any other effects that might possibly be present from exposing the reaction solution to the microfiltration membrane and the microfiltration procedure. Those hypotheses require a knowledge of the composition of the Thermo Scientific Nalgene 0.20 μm syringe filter and its membrane employed herein: the membrane is composed of nylon with a polypropylene housing, stated to be resistant to propylene carbonate, acetone, and hydrocarbon solvents. Nevertheless, the two reasonable alternative hypotheses that we could conceive of for our observed effects of filtration on the kinetics are (a) that the membrane is trapping or otherwise filtering out some of the $[(COD)Ir{\cdot}POM]^{8-}$, thereby lowering the rate due to this hypothesized loss of the precatalyst, or (b) that some poison is leaching out of the membrane, thereby poisoning and slowing the $Ir(0)_n$ catalyst, **B**.

The possibility (a) that filtration was removing some of the $[(COD)Ir{\cdot}POM]^{8-}$ was tested and ruled out by obtaining the UV−visible absorption spectra of the filtered and unfiltered solutions. They are essentially identical (Figure S9 in the SI), disproving the alternative hypothesis that the membrane filtering step is removing a significant portion of the $[(COD)Ir{\cdot}POM]^{8-}$ precatalyst (as would have to be the case to explain the observed 4−7-fold effects seen). In addition, if $[(COD)Ir{\cdot}POM]^{8-}$ were being removed by the filtration step, then one would expect this to be more pronounced at lower concentrations of $[(COD)Ir{\cdot}POM]^{8-}$, so that Figure 2 would have then exhibited a drop off in the rate, $k_{1obs(bimol)}$, at lower $[(COD)Ir{\cdot}POM]^{8-}$, which is not seen (Figure 2, vide supra), further disproving this first alternative hypothesis.

As for (b), the leached poison alternative hypothesis, one would similarly expect a greater relative poisoning at lower $[(COD)Ir{\cdot}POM]^{8-}$. But again, the predicted drop off is not seen (Figure 2, vide supra). In addition, the leached poison hypothesis is further disproven by the fact that filtration of just the solution (without washing the glassware surface with filtered solvent) leaves that solution still fully active (Figure 1, vide supra, curve with the green diamonds, ◇) and hence not poisoned. And, as already mentioned, Figure 3 further verifies this general result because a solution with added alumina dust that is filtered retains its full activity and is also not poisoned at all (Figure 3, vide supra, curve with the pink circles, ○). In short, the two alternative explanations for the observed rate-decreasing effects of filtration that we could conceive of are hereby disproven.

It Must Be Dust! The evidence that the filterable component is dust is, then, mostly indirect except for the optical microscopy and arguably the general results of the 10 DLS experiments but is still compelling because (i) dust is physically omnipresent; (ii) filtration should remove the dust and appears to do so; (iii) we can detect dust and its removal by optical microscopy and to some extent DLS as well; (iv) added authentic dust has the expected nucleation rate-restoring effect; (v) dust effects on particle formation have a precedent;[31−36,42,43] and (vi) the only two reasonable alternative hypotheses we can think of that might have explained the filtration effect a different way have been disproven. We conclude that the filterable component that has the nucleation rate-enhancing agent *must be dust*!

An Important Synthetic and Mechanistic Finding: A Significant Narrowing Effect of Simple Microfiltration on the Final $Ir(0)_n$ Nanoparticle Size Distribution. Because filtration has a noticeable effect on the Ir(0) nanoparticle formation kinetics, we reasoned that filtration must have some effect on the size and size distribution of the $Ir(0)_n$ nanoparticles, the only questions being whether that effect would be readily detectable. Because we were not expecting a very dramatic effect, these studies were done late as part of the present study. The magnitude of the observed effect, on especially the resultant nanoparticle size distribution, surprised us.

First, as a control using the normal unfiltered precatalyst solution and otherwise standard conditions, a TEM of what proved to be 1.74 ± 0.33 nm (±19%) average diameter $Ir(0)_{\sim 200}$ nanoparticles was obtained (Figure 4a). The nanoparticles are a bit smaller than the historically closer to 2.0(±0.3) nm $Ir(0)_{\sim 300}$ nanoparticles shown in Scheme 1, but our experience is that samples easily varying by ±100 Ir(0) atoms can be seen depending on the precise conditions and in any given individual nanoparticle syntheses,[8,11,12,22] a major factor apparently being the amount of filterable component such as dust in the system (vide infra)!

Very interestingly and importantly, $Ir(0)_n$ nanoparticles formed under otherwise identical conditions, except using the microfiltration protocol on the precatalyst solution combined with rinsing of the glassware surfaces with filtered solution, yield a distribution of 1.96 ± 0.16 nm (±8%) $Ir(0)_{\sim 300}$ nanoparticles (Figure 4b). That is, simply adding filtration to the nanoparticle synthesis protocol has increased the average size some, as expected for the slowing of the nucleation rate constant while the autocatalytic growth constant remained the same, *but more importantly narrowed the distribution by a factor of 2.4 to a rather remarkable, near-record narrow* (vide infra) *±8% dispersion for such a self-assembly nanoparticle synthesis*! Because nanoparticle properties invariably are dependent on their size and size distribution of the nanoparticles, this is a significant synthetic as well as mechanistic result!

The synthesis of $Ir(0)_n$ nanoparticles with a relatively narrow ±8% dispersion by a simple self-assembly reaction at room temperature, under otherwise straightforward, nonspecialized conditions, is near the record for any metal(0) nanoparticle self-assembly syntheses and, for that matter, any nanoparticle synthesis not involving chromatographic methods (i.e., as in atom-precise Au_n nanoclusters) as the literature cited next demonstrates. A 2014 paper reporting an optimized Turkevich-type synthesis would appear for the record for a self-assembly synthesis and without any chromatographic separation steps, making $Au(0)_n$ nanoparticles with dispersions as narrow as 5−8%.[61] Even the better synthesis methods at size control for a broad range of nanoparticle materials such as micellar-templated syntheses,[62−65] seeded methods,[66] dendrimer methods,[67,68] or the famous Stöber process[69,70] (and other metal-oxide particle *self-assembly* syntheses[71]) yield dispersions that are, respectively, ±5%,[62−65] ≥±6−10%,[66] ≥±14%,[67,68] and ±5%.[69,70]

Additionally, we can now go back to Matijević's classic study of determining the size distribution of self-assembled S_n sols[39]

DOI: 10.1021/acs.langmuir.7b01219
Langmuir 2017, 33, 6550−6562

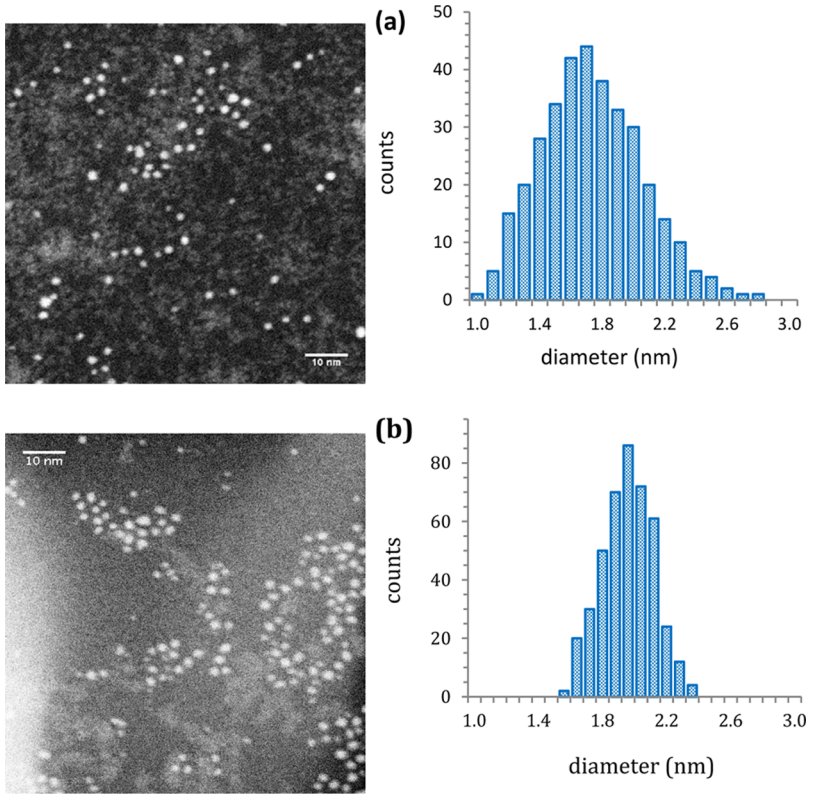

Figure 4. Bright-field STEM images (left) and the corresponding particle size histograms (right) of $Ir(0)_n$ nanoparticles formed under standard conditions of cyclohexene hydrogenation starting with 1.2 mM $[(Bu_4N)_5Na_3(1,5\text{-COD})Ir{\cdot}P_2W_{15}Nb_3O_{62}]$ precursor solution in pyropylene carbonate at 22.0 ± 0.1 °C at an initial H_2 pressure of 40 ± 1 psig: (a) without filtration and (b) after filtration and rinsing of the glass reactor with the filtered propylene carbonate solvent. In constructing the histograms, 347 and 431 nontouching particles were counted, respectively. The mean diameter of Ir(0) nanoparticles is 1.74 ± 0.33 nm for (a) and 1.96 ± 0.16 for (b), corresponding to $Ir(0)_{\sim 200}$ and $Ir(0)_{\sim 300}$, respectively.[60]

in which he carefully controlled multiple experimental parameters of his system and suggest that the dust-removal step he employed was likely more important than could be previously appreciated. Recall that Matijević and co-workers observed a 2-fold size-dispersion narrowing from his synthesis procedure to 0.48(±0.04) μm or ±8% (for 95% of their particles)[39] in comparison to prior work that had a 0.51(±0.08) μm or ±16% dispersion of particles (again for 95% of those particles) for an otherwise similar synthesis.[41] Intriguingly, that 2-fold narrowing in the S_n system is not far off from the 2.4-fold narrowing we see for our present $Ir(0)_n$ nanoparticle system. However, whether this is just coincidence or a more common finding must await the results of studies of additional systems and conditions.

Next, one can ask, do the observed kinetics explain the observed size narrowing? The answer would appear to be yes: the key appears to be the reduction of the (average[11,12,22]) rate constant for slow, continuous nucleation $k_{1obs(bimol)}$ while simultaneously keeping the (average[11,12,22]) autocatalytic surface-growth rate constant $k_{2obs(bimol)}$ the same by lowering the dust content by microfiltration. The larger $k_{2obs(bimol)}/k_{1obs(bimol)}$ ratio means a greater separation of nucleation and growth in time, which in turn predicts a narrower nanoparticle size dispersion.[72]

Overall, then, noteworthy insights from the present studies in comparison to any prior work in the nucleation and growth literature across nature are, to our knowledge, our combined results of (i) the size-narrowing effect of a simple microfiltration step,[39] plus (ii) our measurement of both nucleation and autocatalytic growth rate constants showing that only the nucleation rate constant, $k_{1obs(bimol)}$, is influenced by microfiltration within experimental error, and then also (iii) the insight that it is the reduction in slow, continuous nucleation $k_{1obs(bimol)}$, while keeping the autocatalytic surface growth $k_{2obs(bimol)}$ the same, that can account for the observed size-dispersion narrowing effect. One very interesting set of experiments will be to perform nanoparticle syntheses under increasingly better Clean Room levels and determine if the size dispersions become increasingly narrower. Also, what is the limit of the narrowest size dispersion that can be achieved from any self-assembly synthesis analogous to the $Ir(0)_n$ nanoparticle synthesis studied herein?

Question of the More Precise, Intimate Mechanism. The results presented beg the question of what is the more intimate mechanism behind the observed effects of dust? Is it the recently discovered alternative termolecular mechanism and its implied kinetically effective nucleus (KEN),[12] previously of nominal composition[22] $\{Ir_3H_{2x}POM\}^{6-}$ but now upgraded by the observed effect of dust to something akin to $\{(Ir_3H_{2x}POM^{6-})\cdot dust\}$? Can that account for the observed kinetic effects on nucleation? Overall, do the observed effects of filtration and dust removal make physical sense for the present $[(COD)Ir{\cdot}POM]^{8-}$ precatalyst plus H_2 nanoparticle formation system?

To begin to address the question of the more intimate mechanism, we analyzed the $k_{1obs(bimol)}$ vs $[(COD)Ir{\cdot}POM]^{8-}$ concentration data back in Figure 2 the same way we did recently to determine if any evidence for a change in

DOI: 10.1021/acs.langmuir.7b01219
Langmuir 2017, 33, 6550−6562

mechanism could be discerned.[22] As Figure S10 and the discussion therewith show, no evidence for a change in mechanism is apparent at this time based on the available data. The alternative termolecular mechanism found recently[22] appears to be consistent with the current kinetics data, thereby implying as one hypothesis going forward a KEN when dust is present of composition something like $\{(Ir_3H_{2x}POM^{6-})\cdot dust\}$. Further, speculative discussions of how dust may be having its effects in the present system, as well as the needed additional studies especially of other, carefully designed systems, are provided in the SI for the interested reader.

CONCLUSIONS

The most important conclusions and insights from the present study of the effects of dust on the nucleation kinetics of $Ir(0)_n$ nanoparticle formation, under the condition employed, are the following:

(1) The most remarkable effect of adding a 0.20 μm filtration step is seen in the narrowing of the size distribution of the resulting $Ir(0)_n$ nanoparticles: a decrease in the size dispersity by a factor of 2.4 from ±19% to ±8% is observed after simple microfiltration of the reaction solution prior to the H_2 reduction step that yields the $Ir(0)_n$ nanoparticles! This is the first demonstration that a simple filtration step can have a sizable effect on a transition-metal nanoparticle final size distribution from a self-assembly synthesis involving (slow and continuous,[11] second-order[12]) nucleation and (autocatalytic surface[11]) growth. The resulting ±8% narrowness of the size distribution is near the record, ±5−8%, for any reported simple self-assembly synthesis of metal(0) or other nanoparticles.

(2) The nucleation apparent rate constant $k_{1obs(bimol)}$ is slowed by a factor of ∼5 to ∼7.6 depending on the precise experiment and its conditions following the filtration of the precatalyst solution using a 0.20 μm filter and rinsing the glassware surface with 0.20 μm of filtered propylene carbonate solvent. Both steps are necessary to see the rate-decreasing effect; just filtering the solution, but not rinsing the glassware surface, has no detectable effect on the (then still faster) nucleation rate. The autocatalytic growth rate constant, $k_{2obs(bimol)}$, remains unchanged within experimental error after the prefiltration step.

(3) The narrower size distribution can be accounted for by the slowed nucleation rate constant, $k_{1obs(bimol)}$, yet unchanged autocatalytic growth rate constant, $k_{2obs(bimol)}$, that is by the increased ratio of $k_{2obs(bimol)}/k_{1obs(bimol)}$ that further separates nucleation from growth in time for filtered vs unfiltered solutions. Noteworthy here is that this key effect of slowed nucleation is the antithesis of both classical nucleation theory[23] (CNT) and its assumed burst nucleation from supersaturated solution as well as from LaMer's mechanism[40] that also assumes CNT and burst nucleation. Synthetically slowed nucleation is additionally conceptually opposite of the valuable hot injection methods for selected nanoparticle syntheses. That said, the present results suggest that checking hot injection systems for the ratio of their nucleation vs growth rate constants, as a function of temperature, would be of mechanistic interest.

(4) Five lines of evidence indicate that the filterable component of the solution, which has nucleation rate-enhancing and size-dispersion broadening effects, is dust. This conclusion is, in turn, consistent with and supportive of the literature indicating that both dust and its heterogeneous nucleation pathways are likely omnipresent[31−36,42,43] and kinetically often dominant.[29−36,42,43] In the present example, the main effect seems to come from primarily inorganic dust, a tentative working hypothesis meriting further study.

(5) An important conclusion that follows from this work and that is supported by our prior paper[12] is that many if not the majority of theoretical as well as experimental studies of nucleation across nature that use classical (homogeneous) nucleation theory[23,24] (CNT), either as their starting point or in the interpretation of their data, would appear to be fundamentally flawed because they and at least the original, homogeneous nucleation formulation of CNT[23] "have no provision for the presence of dust".[73] CNT in at least its unmodified, original, and again homogeneous nucleation form would appear to be simply inappropriate for experimental nucleation growth and agglomeration systems not performed in a class 9 Clean Room[50] and, as far as we can tell, for any strongly bonded[12] systems.

(6) Even if studies are performed in a class 9 Clean Room, one will still have to consider the possible effects of, by definition,[51] up to ≤35 particles/ft^3 of 0.1 μm diameter and ≤7.5 particles/ft^3 of 0.2 μm diameter.[50,51] In this regard, repetition of the important study by Kulkarni and co-workers,[42] but now in the best possible clean-room environment, is of considerable fundamental interest in our view. Is true, bona fide homogeneous nucleation ever observable? It is noteworthy that this question was first asked in the late 1800s.[16]

(7) Further studies will be required to test and better understand the more intimate mechanism by which dust is having its effects in the present and other carefully designed and chosen systems. Can the current hypothesis of a KEN of nominal composition $\{(Ir_3H_{2x}POM^{6-})\cdot dust\}$ withstand further experimental testing? Does dust typically actually have a surface charge something like dust^{z-} so that effects in at least systems such as our $[(COD)Ir\cdot POM]^{8-}$ precatalyst may be occurring via cation ion exchange or ion-pairing effects as speculation provided in the SI postulates? Studies of other deliberately added types of inorganic dust, notably those back in Table 1, as well as organic dust on nucleation kinetics and resultant size distributions are other, additional studies meriting future effort.

(8) Finally, the dominant hypothesis going forward for nucleation studies anywhere in nature where dust is (omni)-present should be that dust is a kinetically important component of both the nucleation process and the observed particle size and size distribution.

EXPERIMENTAL SECTION

The experimental details are provided in the Supporting Information.

ASSOCIATED CONTENT

Supporting Information

The Supporting Information is available free of charge on the ACS Publications website at DOI: 10.1021/acs.langmuir.7b01219.

Supporting Information is available providing: Plots showing the effect of using a silanized glass reactor on the nucleation kinetics, $k_{2obs(bimol)}$ vs the precatalyst concentration, and $k_{2obs(bimol)}$ vs $k_{1obs(bimol)}$ for Ir(0) nanoparticle formation from an unfiltered or filtered precatalyst solution. Attempt to detect adventitious dust by light scattering. DLS intensity vs particle size graphs taken from the precatalyst solution and from the unfiltered or filtered propylene carbonate solvent.

DOI: 10.1021/acs.langmuir.7b01219
Langmuir 2017, 33, 6550−6562

Attempted experiment with carbon dust and related kinetics curves. Optical microscopy images taken from the surface of a thin glass coverslip prerinsed with propylene carbonate solvent and from the surface of glass coverslip with and without carbon dust. Nucleation and growth kinetic data and controls for the carbon dust experiments. UV−vis electronic absorption spectra taken from the unfiltered or filtered precatalyst solution. Sources contributing to the large variation and errors in nucleation rate constants. Effect of dust on $k_{2obs(bimol)}$. Initial look at the more intimate mechanism of nucleation. Plot of $k_{1obs(bimol)}$ vs initial concentration of precursor. Experimental section and details. (PDF)

AUTHOR INFORMATION

Corresponding Author

*E-mail: Richard.Finke@colostate.edu.

ORCID

Richard G. Finke: 0000-0002-3668-7903

Notes

The authors declare no competing financial interest.

ACKNOWLEDGMENTS

This work was supported at Colorado State University by the U.S. Department of Energy (DOE), Office of Science, Office of Basic Energy Sciences, Division of Chemical Sciences, Geosciences & Biosciences, via DOE grant SE-FG402-03ER15453. The authors thank Barbara Bernstein for her expert assistance in taking optical microscopy images.

REFERENCES

(1) Kashchiev, D. *Nucleation: Basic Theory with Applications*; Butterworth-Heinemann: Oxford, U.K., 2000.

(2) Zhang, T. H.; Liu, X. Y. Nucleation: what happens at the initial stage? *Angew. Chem., Int. Ed.* **2009**, *48*, 1308−1312.

(3) Sipilä, M.; Berndt, T.; Petäjä, T.; Brus, D.; Vanhanen, J.; Stratmann, F.; Patokoski, J.; Mauldin, R. L.; Hyvärinen, A.-P.; Lihavainen, H.; Kulmala, M. The role of sulfuric acid in atmospheric nucleation. *Science* **2010**, *327*, 1243−1246.

(4) Chen, S.; Ferrone, F. A.; Wetzel, R. Huntington's disease age-of-onset linked to polyglutamine aggregation nucleation. *Proc. Natl. Acad. Sci. U. S. A.* **2002**, *99*, 11884−11889.

(5) Dauer, W.; Przedborski, S. Parkinson's disease: mechanisms and models. *Neuron* **2003**, *39*, 889−909.

(6) Thanh, N. T. K.; Maclean, N.; Mahiddine, S. Mechanisms of Nucleation and Growth of Nanoparticles in Solution. *Chem. Rev.* **2014**, *114*, 7610−7630.

(7) For a critical review of transition-metal nanoparticle stabilizers, see Ott, L. S.; Finke, R. G. Transition-metal nanocluster stabilization for catalysis: A critical review of ranking methods and putative stabilizers. *Coord. Chem. Rev.* **2007**, *251*, 1075−1100.

(8) Lin, Y.; Finke, R. G. Novel Polyoxoanion- and Bu_4N^+-Stabilized, Isolable, and Redissolvable, 20−30 Å $Ir_{300-900}$ Nanoclusters: The Kinetically Controlled Synthesis, Characterization, and Mechanism of Formation of Organic Solvent-Soluble, Reproducible Size, and Reproducible Catalytic Activity Metal Nanoclusters. *J. Am. Chem. Soc.* **1994**, *116*, 8335−8353.

(9) Lin, Y.; Finke, R. G. A More General Approach to Distinguishing "Homogeneous" from "Heterogeneous" Catalysis: Discovery of Polyoxoanion- and Bu_4N^+-Stabilized, Isolable and Redissolvable, High-Reactivity $Ir_{\sim 190-450}$ Nanocluster Catalysts. *Inorg. Chem.* **1994**, *33*, 4891−4910.

(10) Aiken, J. D., III; Lin, Y.; Finke, R. G. A perspective on nanocluster catalysis: polyoxoanion and $(n\text{-}C_4H_9)_4N^+$ stabilized $Ir(0)_{\sim 300}$ nanocluster 'soluble heterogeneous catalysts. *J. Mol. Catal. A: Chem.* **1996**, *114*, 29−51.

(11) Watzky, M. A.; Finke, R. G. Transition Metal Nanocluster Formation Kinetic and Mechanistic Studies. A New Mechanism When Hydrogen Is the Reductant: Slow, Continuous Nucleation and Fast Autocatalytic Surface Growth. *J. Am. Chem. Soc.* **1997**, *119*, 10382−10400.

(12) Laxson, W. W.; Finke, R. G. Nucleation is Second Order: An Apparent Kinetically Effective Nucleus of Two for $Ir(0)_n$ Nanoparticle Formation from $[(1,5\text{-COD})Ir^{I}\cdot P_2W_{15}Nb_3O_{62}]^{8-}$Plus Hydrogen. *J. Am. Chem. Soc.* **2014**, *136*, 17601−17615 and references therein, for example to Classical Nucleation Theory..

(13) Hornstein, B. J.; Finke, R. G. Transition-Metal Nanocluster Kinetic and Mechanistic Studies Emphasizing Nanocluster Agglomeration: Demonstration of a Kinetic Method That Allows Monitoring of All Three Phases of Nanocluster Formation and Aging. *Chem. Mater.* **2004**, *16*, 139−150.

(14) Besson, C.; Finney, E. E.; Finke, R. G. A Mechanism for Transition-Metal Nanoparticle Self-Assembly. *J. Am. Chem. Soc.* **2005**, *127*, 8179−8184.

(15) Besson, C.; Finney, E. E.; Finke, R. G. Nanocluster Nucleation, Growth, and Then Agglomeration Kinetic and Mechanistic Studies: A More General, Four-Step Mechanism Involving Double Autocatalysis. *Chem. Mater.* **2005**, *17*, 4925−4938.

(16) Finney, E. E.; Finke, R. G. The Four-Step, Double-Autocatalytic Mechanism for Transition-Metal Nanocluster Nucleation, Growth, and Then Agglomeration: Metal, Ligand, Concentration, Temperature, and Solvent Dependency Studies. *Chem. Mater.* **2008**, *20*, 1956−1970.

(17) Finney, E. E.; Finke, R. G. Nanocluster nucleation and growth kinetic and mechanistic studies: A review emphasizing transition-metal nanoclusters. *J. Colloid Interface Sci.* **2008**, *317*, 351−374.

(18) Ott, L. S.; Finke, R. G. Transition-Metal Nanocluster Stabilization versus Agglomeration Fundamental Studies: Measurement of the Two Types of Rate Constants for Agglomeration Plus Their Activation Parameters under Catalytic Conditions. *Chem. Mater.* **2008**, *20*, 2592−2601.

(19) Finney, E. E.; Finke, R. G. Fitting and Interpreting Transition-Metal Nanocluster Formation and Other Sigmoidal-Appearing Kinetic Data: A More Thorough Testing of Dispersive Kinetic vs Chemical-Mechanism-Based Equations and Treatments for 4-Step Type Kinetic Data. *Chem. Mater.* **2009**, *21*, 4468−4479.

(20) Finney, E. E.; Finke, R. G. Is There a Minimal Chemical Mechanism Underlying Classical Avrami-Erofe'ev Treatments of Phase-Transformation Kinetic Data? *Chem. Mater.* **2009**, *21*, 4692−4705.

(21) Finney, E. E.; Shields, S. P.; Buhro, W. E.; Finke, R. G. Gold Nanocluster Agglomeration Kinetic Studies: Evidence for Parallel Bimolecular Plus Autocatalytic Agglomeration Pathways as a Mechanism-Based Alternative to an Avrami-Based Analysis. *Chem. Mater.* **2012**, *24*, 1718−1725.

(22) Özkar, S.; Finke, R. G. Nanoparticle Nucleation is Termolecular and Involves Hydrogen: Evidence for a Kinetically Effective Nucleus of Three, $\{Ir_3H_{2x}\cdot P_2W_{15}Nb_3O_{62}\}^{6-}$, in $Ir(0)_n$ Nanoparticle Formation From $[(1,5\text{-COD})IrI\cdot P_2W_{15}Nb_3O_{62}]^{8-}$ Plus Hydrogen. *J. Am. Chem. Soc.* **2017**, *139*, 5444−5457.

(23) Volmer, M.; Weber, A. Keimbildung in Ubersattigten Gebilden (Nucleation in supersaturated systems). *Z. Phys. Chem.* **1926**, *119*, 277−301.

(24) Volmer, M.; Kinetik der Phasenbildung, T. Verlag von Theodor Steinkopff, Leipzig, 1939.

(25) Becker, R.; Döring, W. Kinetische Behandlung der Keimbildung in übersättigten Dämpfen. *Ann. Phys.* **1935**, *416*, 719−752.

(26) Rusyniak, M.; Abdelsayed, V.; Campbell, J.; El-Shall, M. S. Vapor Phase Homogeneous Nucleation of Higher Alkanes: Dodecane, Hexadecane, and Octadecane. 1. Critical Supersaturation and Nucleation Rate Measurements. *J. Phys. Chem. B* **2001**, *105*, 11866−11872.

DOI: 10.1021/acs.langmuir.7b01219
Langmuir 2017, 33, 6550−6562

(27) Rusyniak, M.; El-Shall, M. S. Vapor Phase Homogeneous Nucleation of Higher Alkanes: Dodecane, Hexadecane, and Octadecane. 2. Corresponding States and Scaling Law Analysis. *J. Phys. Chem. B* **2001**, *105*, 11873−11879.
(28) Abedalsayed, V.; Ibrahim, Y.; Rabeony; El-Shall, M. S. Fluoroalcohols as nucleating agents in supersaturated vapors: Efficient clustering with water in the vapor phase. *J. Chem. Phys.* **2001**, *115*, 2897.
(29) Granasy, L.; Podmaniczky, F.; Toth, G. I.; Tegze, G.; Pusztai, T. Heterogeneous nucleation of/on nanoparticles: a density functional study using the phase-field crystal model. *Chem. Soc. Rev.* **2014**, *43*, 2159−2173.
(30) Strey, R.; Wagner, P. E.; Viisanen, Y. The Problem of Measuring Homogeneous Nucleation Rates and the Molecular Contents of Nuclei: Progress in the Form of Nucleation Pulse Measurements. *J. Phys. Chem.* **1994**, *98*, 7748−7758.
(31) Spurny, K. R. Atmospheric Condensation Nuclei P. J. Coulier 1875 and J. Aitken 1880 (Historical Review). *Aerosol Sci. Technol.* **2000**, *32*, 243−248.
(32) Coulier, P. J. Note sur une nouvelle propriete de l'air, J. *J. de Pharmacie et de Chimie, Paris, Ser.* **1875**, *4*, 165−173.
(33) Aitken, J. On the dust, fog, and clouds. *Proc. R. Soc. Edinburgh* **1882**, *11*, 14−18.
(34) Aitken, J. On the numbers of dust particles in the atmosphere in certain places in Great Britain and on the continent, with remarks on the relation between the amount of dust and meteorological phenomena. *Trans. - R. Soc. Edinburgh* **1889**, *35*, 1−19.
(35) Aitken, J. On improvements in the apparatus for counting the dust particles in the atmosphere. *Proc. R. Soc. Edinburgh* **1890**, *16*, 135−172.
(36) Aitken, J. On a simple pocket dust-counter. *Proc. R. Soc. Edinburgh* **1892**, *18*, 39−52.
(37) Wilson, C. T. R. Condensation of water vapour in the presence of dust-free air and other gases. *Philos. Trans. R. Soc., A* **1897**, *189*, 265−307.
(38) Turkevich, J.; Stevenson, P. C.; Hiller, J. A study of the nucleation and growth processes in the synthesis of colloidal gold. *Discuss. Faraday Soc.* **1951**, *11*, 55−75.
(39) Kerker, M.; Daby, E.; Cohen, G. L.; Kratohvil, J. P.; Matijevic, E. Particle size distribution in LaMer sulfur sols. *J. Phys. Chem.* **1963**, *67*, 2105−2111.
(40) LaMer, V. K.; Dinegar, R. H. Theory, Production and Mechanism of Formation of Monodispersed Hydrosols. *J. Am. Chem. Soc.* **1950**, *72*, 4847.
(41) Petro, A. J. Particle size distribution in monodisperse sulfur hydrosols. *J. Phys. Chem.* **1960**, *64*, 1508−1511.
(42) Kulkarni, S. A.; Kadam, S. S.; Meekes, H.; Stankiewicz, A. L.; ter Horst, J. H. Crystal nucleation kinetics from induction times and metastable zone widths. *Cryst. Growth Des.* **2013**, *13*, 2435−2440.
(43) For a lead reference, see Kulkarni, G.; Sanders, C.; Zhang, K.; Liu, X.; Zhao, C. Ice nucleation of bare and sulfuric acid-coated mineral dust particles and implication for cloud properties. *J. Geophys. Res.: Atmos* **2014**, *119*, 9993−10011.
(44) Poole, J. A.; Romberger, D. J. Immunological and inflammatory responses to organic dust in agriculture. *Curr. Opin. Allergy Clin. Immunol.* **2012**, *12*, 126−132.
(45) Seifert, S. A.; Von Essen, S.; Jacobitz, K.; Crouch, R.; Lintner, C. P. Organic dust toxic syndrome: a review. *J. Toxicol., Clin. Toxicol.* **2003**, *41*, 185−193.
(46) Pelley, J. Tracing the Chemistry of Household Dust. *C&EN*, **2017**, *February 13*, 18−21.
(47) Widegren, J. A.; Bennett, M. A.; Finke, R. G. Is It Homogeneous or Heterogeneous Catalysis? Identification of Bulk Ruthenium Metal as the True Catalyst in Benzene Hydrogenations Starting With the Monometallic Precursor, Ru(II) $(\eta^6\text{-}C_6Me_6)(OAc)_2$, Plus Kinetic Characterization of the Heterogeneous Nucleation, Then Autocatalytic Surface-Growth Mechanism of Metal Film Formation. *J. Am. Chem. Soc.* **2003**, *125*, 10301−10310.
(48) One could, however, and if desired use the first-order FW two-step mechanism for the fits to yield k_{1obs} and then derive $k_{1obs(bimol)}$ from that via identity $k_{1obs(bimol)} = k_{1obs}[A_0]$, which is true because $[A_0]$ is constant to >99.99% during the induction period.[12] Indeed and as discussed elsewhere, the first-order FW two-step mechanism hides higher-order nucleation mechanisms until and unless they are specifically tested for, as we did for the $Ir(0)_n$ nanoparticle system, where a net second-order nucleation proved to be present.[12]
(49) Ott, L. S.; Finke, R. G. Supersensitivity of transition-metal nanoparticle formation to initial precursor concentration and reaction temperature: Understanding its origins. *J. Nanosci. Nanotechnol.* **2008**, *8*, 1551−1556. This paper shows how sensitive the $Ir(0)_n$ (and by implication other, similar) nanoparticle formation systems can be to the precise reaction conditions. It was speculated in that paper the sensitivity of the reaction to the prior dissociative equilibrium and its $K_{Diss(apparent)}$ value described in our more recent publication.[22]
(50) An ISO Clean Room 1 contains 35 000 000 particles per cubic meter in the size range of 0.5 μm and larger in diameter. Even the best, class 9 Clean Room can still have, by definition, ≤35 particles/ft^3 of 0.1 μm diameter and ≤7.5 particles/ft^3 of 0.2 μm diameter. ISO/TC 209 Clean Rooms and associated controlled environments: http://www.iso.org/iso/catalogue_detail.htm?csnumber=25052.
(51) Hong, S.; Berndt, J.; Winter, J. Study of Particle Formation and its Applications in Ar/CH_4 and Ar/C_2H_2 Mixtures. *AIP Conf. Proc.* **2002**, *649*, 305−308.
(52) Rudakov, D. L.; Yu, J. H.; Boedo, J. A.; Hollmann, E. M.; Krasheninnikov, S. I.; Moyer, R. A.; Muller, S. H.; Pigarov, A.; Yu; Rosenberg, M.; Smirnov, R. D.; West, W. P.; Boivin, R. L.; Bray, B. D.; Brooks, N. H.; Hyatt, A. W.; Wong, C. P. C.; Roquemore, A. L.; Skinner, C. H.; Solomon, W. M.; Ratynskaia, S.; Fenstermacher, M. E.; Groth, M.; Lasnier, C. J.; McLean, A. G.; Stangeby, P. C. Dust measurements in tokamaks. *Rev. Sci. Instrum.* **2008**, *79*, 10F303.
(53) Sawada, S.; Kobayashi, K. Dust detection using multiple reflection. *Appl. Opt.* **1991**, *30*, 4966−4971.
(54) Tianhua, L.; Ying, W. Design of indoor dust concentration monitor based on light scattering detection method. *Sci. Res. Essays* **2014**, *9*, 321−324.
(55) Berne, B. J.; Pecora, R. *Dynamic Light Scattering*; Courier Dover Publications: Mineola, NY, 2000.
(56) Berne, B. J.; Pecora, R. Laser Light Scattering from Liquids. *Annu. Rev. Phys. Chem.* **1974**, *25*, 233−253.
(57) Kent, P. D.; Mondloch, J. E.; Finke, R. G. A Four-Step Mechanism for the Formation of Supported-Nanoparticle Heterogenous Catalysts in Contact with Solution: The Conversion of Ir(1,5-COD)Cl/γ-Al_2O_3 to $Ir(0)_{\sim 170}$/γ-Al_2O_3. *J. Am. Chem. Soc.* **2014**, *136*, 1930−1941.
(58) Platt, J. R. Strong Inference. *Science* **1964**, *146*, 347−353.
(59) Chamberlin, T. C. Studies for Students. The Method of Multiple Working Hypotheses. *J. Geol.* **1897**, *5*, 837−848.
(60) The average size of the iridium(0) nanoparticles was estimated on the basis of an assumed fcc structure for iridium: $n = (N_0\rho(4/3)\pi(D/2)^3)/W$,[8] where n is the number of Ir atoms, $N_0 = 6.022 \times 10^{23}$ mol^{-1}, ρ is the room-temperature density of iridium (22.5 g/cm^3),[60] D is the diameter of iridium nanoparticles, and W is the atomic weight of iridium (192.22 g/mol). This calculation yields $Ir_{\sim 195}$ for an average diameter of ∼1.74 nm and $Ir_{\sim 278}$ for average diameters of 1.96 nm . In *CRC Handbook of Chemistry and Physics*, 77th ed.; Lide, D. R., Frederikse, H. P. R., Eds.; CRC Press: Boca Raton, FL, 1996.
(61) Schulz, F.; Homolka, T.; Bastús, N. G.; Puntes, V.; Weller, H.; Vosseyer, T. Little Adjustments Significantly Improve the Turkevich Synthesis of Gold Nanoparticles. *Langmuir* **2014**, *30*, 10779−10784.
(62) Micellar-templated CdSe nanoparticles of 48.5 ± 2.5 Å, $[(CdSe)_{1800\pm250}](SR)_x$ and hence ±5%, are known: Alivisatos, A. P.; Harris, A. L.; Levinos, M. L.; Steigerwald, M. L.; Brus, L. E. Electronic states of semiconductor clusters: homogeneous and inhomogeneous broadening of the optical spectrum. *J. Chem. Phys.* **1988**, *89*, 4001−4011.
(63) ±10% size dispersion nanoparticles of Pt, Pd, Rh, and Ir by a microemulsion method: Boutonnet, M.; Kizling, J.; Stenius, P.; Maire,

DOI: 10.1021/acs.langmuir.7b01219
Langmuir 2017, 33, 6550−6562

G. The preparation of monodisperse colloidal metal particles from microemulsions. *Colloids Surf.* **1982**, *5*, 209−225.
(64) Micellar-templated CdS nanoparticles of 2.1 ± 0.2 nm: Maheshwari, V.; Saraf, R. F. Mineralization of Monodispersed CdS Nanoparticles on Polyelectrolyte Superstructure Forming an Electroluminescent "Necklace-of-Beads. *Langmuir* **2006**, *22*, 8623−8626.
(65) Template synthesis of Au, Pt, and Pd nanoclusters with sizes ≤3 nm: Zhou, Y.; Zeng, H. C. Simultaneous Synthesis and Assembly of Noble Metal Nanoclusters with Variable Micellar Templates. *J. Am. Chem. Soc.* **2014**, *136*, 13805−13817.
(66) Musah, R. A.; Jensen, G. M.; Rosenfeld, R. J.; McRee, D. E.; Goodin, D. B.; Bunte, S. W. Variation in Strength of an Unconventional C−H to O Hydrogen Bond in an Engineered Protein Cavity. *J. Am. Chem. Soc.* **1997**, *119*, 9083−9084.
(67) Dendrimer-encapsulated Pt and Pd nanoparticles with a <14% dispersion: Myers, V. S.; Weir, M. G.; Carino, E. V.; Yancey, D. F.; Pande, S.; Crooks, R. M. Dendrimer-encapsulated nanoparticles: New synthetic and characterization methods and catalytic applications. *Chem. Sci.* **2011**, *2*, 1632−1646.
(68) Lu, Y.; Liu, J. Smart Nanomaterials Inspired by Biology: Dynamic Assembly of Error-Free Nanomaterials in Response to Multiple Chemical and Biological Stimuli*Chem. Industr.* **2007**, *38*, doi: 10.1002/chin.200731261
(69) Stöber, W.; Fink, A.; Bohn, E. Controlled growth of monodisperse silica spheres in the micron size range. *J. Colloid Interface Sci.* **1968**, *26*, 62−69 The impact of such ultranarrow particle size distributions is apparent in the more than 7500 citations this paper has (as of April 1, 2017)..
(70) Giesche, H. Synthesis of monodispersed silica powders I. Particle properties and reaction kinetics. *J. Eur. Ceram. Soc.* **1994**, *14*, 189−204 Dispersions of ±5−6% are the smallest of those reported therein..
(71) Matijević's classic syntheses of $M_aO_b(OH)_c$ and related materials merit mention in any discussion of ultranarrow particle size distributions: Matijević, E. Preparation and properties of uniform size colloids. *Chem. Mater.* **1993**, *5*, 412−426.
(72) Note that one might be tempted to try to correlate the observed standard deviation of $k_{1obs(bimol)}$ (Table 2 and Figure 2) with the narrowed distribution shown in Figure 4, but that would be a logic mistake in our view because the error bars on $k_{1obs(bimol)}$ were determined in the usual way from multiple repeat experiments, whereas the narrowed size distribution in Figure 4b refers to a single nanoparticle formation experiment (which in turn refers to single nucleation $k_{1obs(bimol)}$ and autocatalytic growth $k_{2obs(bimol)}$ rate constants). Moreover, upon filtration the values of the error bars on $k_{1obs(bimol)}$ are a larger, broader percentage of the (smaller) rate constant (±47% vs ± 27% for unfiltered $k_{1obs(bimol)}$) so that the error bars on $k_{1obs(bimol)}$ from multiple experiments are anticorrelated with the smaller, narrower breadth of a size distribution in a single experiment.
(73) Wheeler, M. J.; Bertram, A. K. Deposition nucleation on mineral dust particles: a case against classical nucleation theory with the assumption of a single contact angle. *Atmos. Chem. Phys.* **2012**, *12*, 1189−1201 In this study, the authors tried to account for the effects of ice formation that, experimentally, proved to be a strong function of the dust surface area made available for nucleation. Classical nucleation theory (CNT) was not able to account for the data nor was CNT modified by the assumption of a single contact angle (the single α-model therein) able to account for the authors' data. However, the use of a distribution of contact angles was able to account for the strong effect of added kaolinite or illite mineral dusts[43] on the formation of ice crystals observed by optical microscopy (so, again, really the first observable clusters and not necessarily the desired kinetically effective nucleus[12]). The author's main conclusion was stated as part of their paper's title, "...A Case Against Classical Nucleation Theory With the Assumption of a Single Contact Angle"..

DOI: 10.1021/acs.langmuir.7b01219
Langmuir 2017, 33, 6550−6562